On the influence of statistics on the determination of the mean value of the depth of shower maximum for ultra high energy cosmic ray showers

On the influence of statistics on the determination of the mean value of the depth of shower maximum for ultra high energy cosmic ray showers

A D Supanitsky[1] and G Medina-Tanco[2]

[1] Instituto de Astronomía y Física del Espacio (IAFE), UBA-CONICET, Argentina
[2] Instituto de Ciencias Nucleares, UNAM, Circuito Exterior S/N, Ciudad Universitaria, México D F 04510, Mexico

E-mail: supanitsky@iafe.uba.ar and gmtanco@nucleares.unam.mx

Abstract

The chemical composition of ultra high energy cosmic rays is still uncertain. The latest results obtained by the Pierre Auger Observatory and the HiRes collaboration, concerning the measurement of the mean value and the fluctuations of the atmospheric depth at which the showers reach the maximum development, X_{max}, are inconsistent. From comparison with air shower simulations it can be seen that, while the Auger data may be interpreted as a gradual transition to heavy nuclei for energies larger than ~ 2–3×10^{18} eV, the HiRes data are consistent with a composition dominated by protons. In Wilk and Wlodarczyk (2011 *J. Phys. G: Nucl. Part. Phys*. **38** 085201), it is suggested that a possible explanation for the observed deviation of the mean value of X_{max} from the proton expectation, observed by Auger, could originate in a statistical bias arising from the approximated exponential shape of the X_{max} distribution, combined with the decrease of the number of events as a function of primary energy. In this paper, we consider a better description of the X_{max} distribution and show that the possible bias in the Auger data is at least one order of magnitude smaller than the one obtained when assuming an exponential distribution. Therefore, we conclude that the deviation of the Auger data from the proton expectation is unlikely to be explained by such statistical effect.

(Some figures may appear in colour only in the online journal)

1. Introduction

The nature of the primary cosmic rays is intimately related to the astrophysical objects capable of accelerating these particles to such high energies. Also, propagation in the intergalactic medium depends on the composition, which affects the resulting spectral distribution of the

flux observed on Earth. A knowledge of the composition is also very important for primary energy reconstruction and for anisotropy studies.

One of the most important limitations of composition analysis comes from the lack of knowledge of the hadronic interactions at the highest energies. Composition studies are based on the comparison of experimental data with Monte Carlo simulations of atmospheric cosmic rays showers, which makes use of hadronic interaction models which extrapolate the available low-energy accelerator data to the energies of the cosmic rays.

One of the most sensitive parameters to the mass of the primary cosmic ray is the atmospheric depth at which the showers reach their maximum development. Lighter primaries generate showers that are more penetrating, producing larger values of X_{max}. Also, the fluctuations of this parameter are smaller for heavier nuclei. The Pierre Auger Observatory and the HiRes experiment are able to observe directly the longitudinal development of the showers by means of fluorescence telescopes. Therefore, in both experiments, the X_{max} parameter of each observed shower can be reconstructed from the data taken by the telescopes.

The mean value and the standard deviation of X_{max}, as a function of primary energy, obtained by Auger [2] and HiRes [3] appear to be inconsistent. From the comparison with simulations, the Auger data suggests a transition to heavier nuclei starting at energies of the order of 2–3×10^{18} eV, whereas, the HiRes data are consistent with protons in the same energy range. In [1], a new parameter, the difference between the mean value and the standard deviation of X_{max}, was introduced in order to reconcile the Auger and HiRes results. This new parameter has the advantage of being much less sensitive to the first interaction point than the mean value and the standard deviation separately. From a comparison of the experimental values of this parameter, obtained by Auger and HiRes, with simulated data, they infer that the composition of the cosmic rays is dominated by protons. They say that the energy dependence of the distribution of X_{max}, observed by Auger, seems to be caused by an unexpected change in the depth of the first interaction point, which can be explained by a rapid increase of the cross section and/or increase of the inelasticity. Both possibilities require an abrupt onset of new physics in this energy range, which makes them questionable. They also suggest that the deviation of the distribution of X_{max} from the proton expectation, present in the Auger data, could be originated in the statistical techniques used to analyze the data. In particular, they suggest that the deviation of the mean value of X_{max} from the proton expectation could be explained by a bias originated from the exponential nature of the X_{max} distribution and the decreasing number of events as a function of primary energy.

In this work we show that, considering a better description of the X_{max} distribution, the bias in the determination of the mean value of X_{max} becomes more than one order of magnitude smaller than the one obtained for the exponential distribution. We find that the value of the bias in the last energy bin (the one with the smallest number of events) of the Auger data, published in [2], is $\lesssim 1.5$ g cm^{-2}, which is much smaller than the systematic errors on the determination of the mean value of X_{max} estimated in [2].

2. Numerical approach

Following [1], let us introduce the parameter

$$\xi(N) = 1 - \frac{\text{mode}\left[\bar{X}_{max}^N\right]}{\langle X_{max} \rangle}, \tag{1}$$

where $\langle X_{max} \rangle$ is the mean value of the X_{max} distribution;

$$\bar{X}_{max}^N = \frac{1}{N} \sum_{i=1}^{N} X_{max}^i \tag{2}$$

2

is the sample mean corresponding to samples of size N and mode$[\bar{X}_{max}^N]$ is the value of $\bar{X}_{max}^N$ that occurs most frequently, i.e. the maximum of the distribution function of $\bar{X}_{max}^N$. Therefore, the bias on the determination of $\langle X_{max} \rangle$ appears when a particular realization of the sample mean is equal to the mode of the sample mean distribution function. Note that the sample mean (equation (2)) is an unbiased estimator of the mean of the exponential distribution, i.e. $E[\bar{X}_{max}^N] = \langle X_{max} \rangle$. In [1], it is shown that approximating the X_{max} distribution by an exponential function the parameter $\xi(N)$ is given by $\xi_E(N) = 1/N$.

In order to better describe the distribution of X_{max} two different types of function are considered. They are chosen in such a way that the distribution of $\bar{X}_{max}^N$ can be obtained, at least, in a semi-analytical way. The first function considered is a shifted-Gamma distribution [4]:

$$
P_G(X_{max}) = \begin{cases} \dfrac{(X_{max} - X_0)^{k-1}}{\Gamma(k)\,\tau_X^k} \exp\left(-\dfrac{X_{max} - X_0}{\tau_X}\right) & X_{max} \geqslant X_0 \\ 0 & X_{max} < X_0 \end{cases}, \tag{3}
$$

where $k = 5$ and the other two parameters can be obtained from the mean value and the standard deviation of X_{max},

$$
X_0 = \langle X_{max} \rangle - k\,\tau_X, \tag{4}
$$

$$
\tau_X = \frac{\sigma[X_{max}]}{\sqrt{k}}. \tag{5}
$$

The second function under consideration is the convolution between an exponential function and a Gaussian (exp-Gauss),

$$
\begin{aligned}
P_{EG}(X_{max}) &= \frac{1}{\lambda\sqrt{2\pi}\,\beta} \int_{-\infty}^{X_{max}} du\; \exp\left(-\frac{X_{max} - u}{\lambda}\right) \exp\left(-\frac{(u - \alpha)^2}{2\beta^2}\right) \\
&= \frac{1}{2\lambda} \exp\left(-\frac{X_{max} - \alpha}{\lambda} + \frac{\beta^2}{2\lambda^2}\right) \mathrm{Erfc}\left(\frac{\beta}{\sqrt{2}\lambda} - \frac{X_{max} - \alpha}{\sqrt{2}\beta}\right),
\end{aligned} \tag{6}
$$

where α, β and λ are the fitting parameters and

$$
\mathrm{Erfc}(z) = 1 - \frac{2}{\sqrt{\pi}} \int_0^z dt\; \exp(-t^2/2). \tag{7}
$$

A library of simulated showers was generated by using the program CONEX (v2r2.3) [5]. Monochromatic samples of 10^4 proton showers were generated from $\log(E/eV) = 18$ to $\log(E/eV) = 19.5$ in steps of $\Delta \log(E/eV) = 0.1$. The arrival directions of the showers follow an isotropic distribution, such that the zenith angle is in the interval $[0°, 60°]$. The hadronic interaction models considered are QGSJET-II [6] and EPOS 1.99 [7].
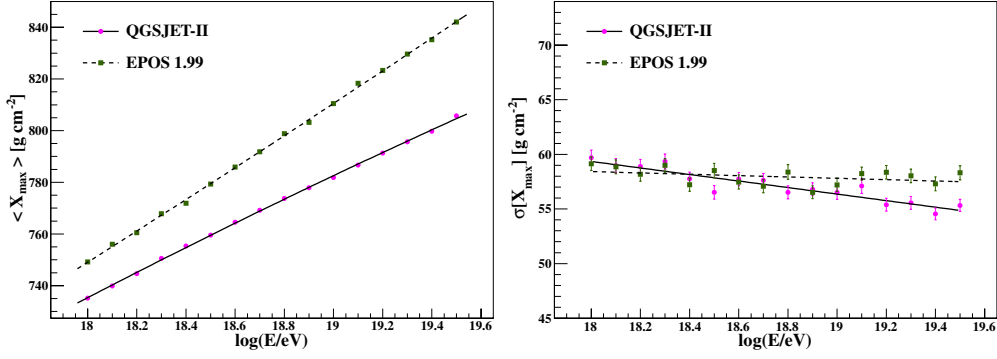
The mean value and the standard deviation (needed for the description of the X_{max} distribution using the shifted-Gamma function) were fitted with a quadratic function and a linear function of $\log(E)$, respectively, i.e.

$$
\langle X_{max} \rangle = A_0 + A_1 \log(E/eV) + A_2 \log^2(E/eV), \tag{8}
$$

$$
\sigma[X_{max}] = B_0 + B_1 \log(E/eV). \tag{9}
$$

Figure 1 shows the simulated data as well as the fits, for both hadronic interaction models considered. The values of the parameters corresponding to equations (8) and (9) are given in table 1.

The distribution functions of X_{max}, for every energy and hadronic interaction model considered, were fitted with the exp-Gauss function, equation (6). The parameters α, β and λ were fitted with linear functions of $\log(E)$, in order to obtain the exp-Gauss representation of

Figure 1. Mean value (left panel) and the standard deviation (right panel) of X_{max} as a function of $\log(E/eV)$ obtained by using CONEX with QGSJET-II and EPOS 1.99 for proton initiated showers. The lines correspond to the fits of the simulated data (see the text for details).

Table 1. Parameters corresponding to the quadratic and linear fits of $\langle X_{max} \rangle$ and $\sigma[X_{max}]$, respectively (see equations (8) and (9)), obtained from simulations for QGSJET-II and EPOS 1.99.

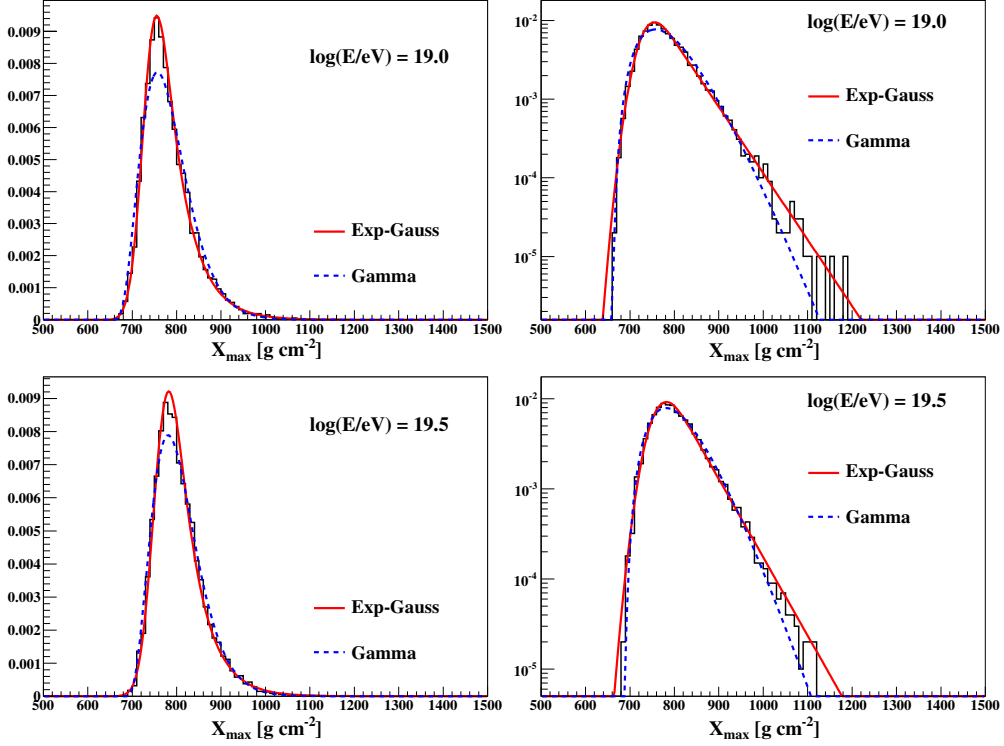|	A_0 (g cm^{-2})	A_1 (g cm^{-2})	A_2 (g cm^{-2})	B_0 (g cm^{-2})	B_1 (g cm^{-2})
QGSJET-II	-826.171	124.198	-2.08037	113.223	-2.99273
EPOS 1.99	80.4419	14.1183	1.27933	69.4862	-0.614616

the X_{max} distribution for every value of energy in the interval $[10^{18}, 10^{19.5}]$ eV, see appendix A for details.

Figure 2 shows the distributions of X_{max}, obtained by using CONEX with QJSJET-II, for $\log(E/eV) = 19$ and $\log(E/eV) = 19.5$. Solid lines correspond to the fits of the simulated data with the exp-Gauss function. The dashed lines correspond to the shifted-Gamma function, equation (3), for which the parameters X_0 and τ_X are obtained by using the expressions of $\langle X_{max} \rangle$ and $\sigma[X_{max}]$ in equations (8) and (9) to calculate X_0 and τ_X from equations (4) and (5), respectively. From the figure, it can be seen that the exp-Gauss function is a better fit to the simulated data than the shifted-Gamma function. It can also be seen that the tail to larger values of X_{max} is slightly overestimated by the exp-Gauss distribution and underestimated by the shifted-Gamma function. Therefore, the distribution function of the universe (samples with $N \rightarrow \infty$) should fall between these two functions.

The distribution of $\bar{X}_{max}^N$ can be calculated by means of the characteristic function, which is defined as the expectation value of $\exp(itX_{max})$, i.e. $\phi_{X_{max}}(t) = E[\exp(itX_{max})]$. It is straightforward to show that the characteristic function of $\bar{X}_{max}^N$ is given by $\phi_{\bar{X}_{max}^N}(t) = [\phi_{X_{max}}(t/N)]^N$ [8].

The characteristic function of the shifted-Gamma distribution is $\phi_{X_{max}}^G(t) = \exp(iX_0 t)(1 - it\tau_X)^{-k}$ and then the characteristic function of $\bar{X}_{max}^N$ is given by $\phi_{\bar{X}_{max}^N}^G(t) = \exp(iX_0 t)(1 - it\tau_X/N)^{-kN}$, which corresponds also to a shifted-Gamma distribution. Therefore, the distribution function of $\bar{X}_{max}^N$ is given by

$$\bar{P}_G(\bar{X}_{max}^N) = \begin{cases} \dfrac{(\bar{X}_{max}^N - X_0)^{Nk-1}}{\Gamma(Nk)\,(\tau_X/N)^{Nk}} \exp\left(-\dfrac{\bar{X}_{max}^N - X_0}{\tau_X/N}\right) & \bar{X}_{max}^N \geqslant X_0 \\ 0 & \bar{X}_{max}^N < X_0 \end{cases} \tag{10}$$

Figure 2. Distributions of X_{max} for proton showers generated by using CONEX with QGSJET-II. Solid lines correspond to the fits of the histograms with the exp-Gauss function, equation (6). The dashed lines correspond to the shifted-Gamma function, equation (3), where the parameters X_0 and τ_X are obtained by using equations (4) and (5), and the fits of $\langle X_{max}\rangle$ and $\sigma[X_{max}]$ as a function of $\log E$ (see text for details).

By using equation (10), it is easy to show that

$$\xi_G(N) = \frac{\sigma[X_{max}]}{\sqrt{k}\,\langle X_{max}\rangle}\,\frac{1}{N}. \tag{11}$$

In this case, ξ is also proportional to $1/N$ but it is suppressed by the ratio between the standard deviation and the mean value of X_{max}. A similar expression is obtained when the distribution function of X_{max} is described by a truncated exponential function, see appendix B for details. The solid line on the left panel of figure 3 corresponds to ξ_G as a function of N for $\log(E/eV) = 19.5$, approximately the mean value of the energy (weighted by the spectrum) for the last bin considered in [2]. Note that the number of events in this bin is 34. From the figure, it can be seen that ξ_G is more than one order of magnitude smaller than the function $1/N$.

The distribution function of X_{max} is affected by the presence of fluctuations introduced by the detectors. The distribution function of $\bar{X}_{max}^N$, including a Gaussian uncertainty on the determination of X_{max} is given by

$$\bar{P}_G^R(\bar{X}_{max}^N) = \frac{\sqrt{N}}{\sqrt{2\pi}\,\sigma_{Rec}} \int_0^\infty dX\,\bar{P}_G(X) \exp\left(-\frac{(\bar{X}_{max}^N - X)^2}{2\sigma_{Rec}^2/N}\right), \tag{12}$$

where σ_{Rec} is the standard deviation of such uncertainty. The mode of this distribution is calculated numerically. Dashed and dash-dotted lines on the left panel of figure 3 correspond
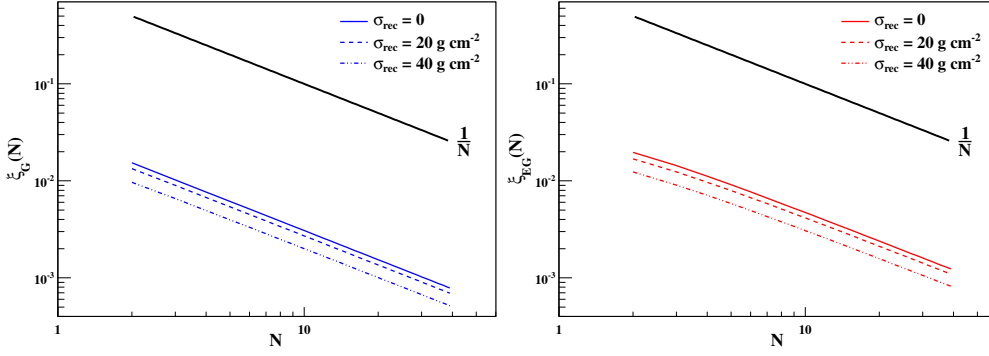
Figure 3. ξ as a function of the sample size N corresponding to proton showers of $\log(E/eV) = 19.5$, obtained for the shifted-Gamma distribution (left panel) and for the exp-Gauss distribution (right panel). Solid lines correspond to the ideal case in which X_{max} is determined without any uncertainty. Dashed and dash-dotted lines correspond to the cases in which there is a Gaussian uncertainty on the determination of X_{max} of $\sigma_{Rec} = 20$ g cm^{-2} and $\sigma_{Rec} = 40$ g cm^{-2}, respectively. The hadronic interaction model used is QGSJET-II.

to parameter $\xi_G(N)$ obtained for $\sigma_{Rec} = 20$ g cm^{-2} and $\sigma_{Rec} = 40$ g cm^{-2}, respectively. When a symmetric uncertainty on the determination of X_{max} is included, the parameter ξ becomes still smaller and decreases for increasing values of the uncertainty. This is due to the fact that ξ is larger for asymmetric distributions, like the exponential, and the convolution of the pure X_{max} distribution with a Gaussian is more symmetric than the original one.

The characteristic function of the exp-Gauss distribution is the product of the characteristic function of the exponential distribution, $(1 - i\lambda t)^{-1}$, with the one corresponding to a Gaussian, $\exp(i\alpha t - \beta^2 t^2/2)$. Then, the characteristic function of $\bar{X}_{max}^N$ is given by

$$\phi_{\bar{X}_{max}^N}^{EG}(t) = \left(1 - i\frac{\lambda}{N}t\right)^{-N} \exp\left(i\alpha t - \frac{\beta^2}{N}t^2/2\right), \tag{13}$$

which corresponds to the convolution of a Gamma distribution with a Gaussian

$$\bar{P}_{EG}(\bar{X}_{max}^N) = \frac{N^{N+1/2}}{\sqrt{2\pi}\beta\lambda^N\Gamma(N)} \int_{-\infty}^{\bar{X}_{max}^N} du\, (\bar{X}_{max}^N - u)^{N-1} \exp\left(-\frac{\bar{X}_{max}^N - u}{\lambda/N}\right)$$
$$\times \exp\left(-\frac{(u-\alpha)^2}{2\beta^2/N}\right). \tag{14}$$

The last integral is calculated numerically in order to obtain the mode of the resultant distribution. The solid line in the right panel of figure 3 shows ξ_{EG} as a function of the sample size for $\log(E/eV) = 19.5$. Note that ξ_G is smaller than ξ_{EG}, this is due to the more extended tail to larger values of the exp-Gauss distribution compared with the corresponding one to the shifted-Gamma distribution. In any case, ξ_{EG} is still about one order of magnitude smaller than $1/N$. As for the case of the Gamma distribution, dashed and dashed-dotted lines correspond to $\sigma_{Rec} = 20$ g cm^{-2} and $\sigma_{Rec} = 40$ g cm^{-2}, respectively. In this case, the effect of the uncertainty on the determination of X_{max} is included in $\bar{P}_{EG}$ just by replacing the parameter β by $\tilde{\beta} = \sqrt{\beta^2 + \sigma_{Rec}^2}$. As expected, the curves that include the uncertainty on the determination of X_{max} fall below the one corresponding to the ideal case.

The left panel of figure 4 shows the parameter ξ as a function of energy corresponding to the number of events in each energy bin taken from [2], for the case in which there is no uncertainty on the determination of X_{max} (which gives larger value of ξ, as shown before). The energy assigned to the ith bin, used to calculate ξ, corresponds to the mean value of the energy
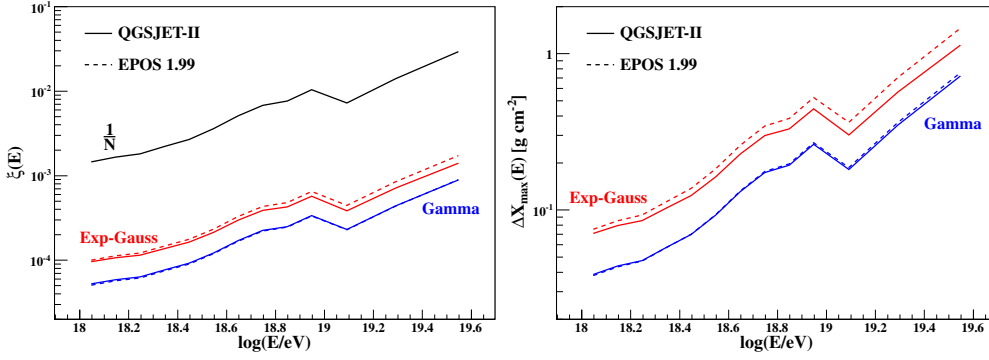
Figure 4. ξ (left panel) and ΔX_{max} (right panel) as a function of $\log(E/eV)$, for the statistics of the Auger data of [2]. Solid lines correspond to QGSJET-II and dashed lines correspond EPOS 1.99.

in the bin weighted by the broken power-law fit of the cosmic rays energy spectrum, $J(E)$, of [9],

$$\langle E_i \rangle = \frac{\int_{E_i^L}^{E_i^U} dE \, E J(E)}{\int_{E_i^L}^{E_i^U} dE \, J(E)}, \tag{15}$$

where E_i^L and E_i^U are the lower and upper limits of the ith bin. It can be seen that the values of ξ, obtained by using the exp-Gauss distribution and the shifted-Gamma distribution, are more than one order of magnitude smaller than the corresponding one for the exponential distribution, in the whole energy range and for both hadronic interaction models considered. As in the previous calculation, ξ_G results are smaller than ξ_{EG}. In fact, the ξ curve corresponding to the true distribution of X_{max} should fall between the curves corresponding to the exp-Gauss and the shifted-Gamma representation of the X_{max} distribution.

The right panel of figure 4 shows the parameter $\Delta X_{max} = \langle X_{max} \rangle \xi$ which gives the grammage of the shift suffered by $\langle X_{max} \rangle$ if $\bar{X}_{max}^N$ takes the value of the mode of its distribution. It can be seen, that for the last energy bin, the one with 34 events, ΔX_{max} is $\lesssim 1.5 \, g \, cm^{-2}$, which is much smaller than the systematic uncertainties on the determination of $\langle X_{max} \rangle$ estimated in [2].

The energy bins considered in the analysis of [2] have a width of $\Delta \log(E/eV) = 0.1$ in the energy range from $E = 10^{18}$ eV to $E = 10^{19}$ eV. Between $E = 10^{19}$ eV and $E = 10^{19.4}$ eV, $\Delta \log(E/eV)$ changes to 0.2 and the last bin corresponds to $E \geqslant 10^{19.4}$ eV. Therefore, the number of events per bin decreases in the energy range from $E = 10^{18}$ eV to $E = 10^{19}$ eV, it increases from 96 in the bin $[10^{18.9}, 10^{19}]$ eV to 138 in the bin $[10^{19}, 10^{19.2}]$ eV and then, it decreases for the last two bins. This change in the bin width generates the structure around $E \cong 10^{19.1}$ eV seen on the curves of figure 4.

Note that ξ_{EG} calculated by using EPOS 1.99 is larger than the corresponding one for QGSJET-II, this is due to the fact that the X_{max} distributions obtained with EPOS 1.99 are more asymmetric (increase faster, coming from small values of X_{max}, and have a more extended tail) than the corresponding ones to QGSJET-II.

Concerning iron showers, it can be seen that ξ takes smaller values than the ones for protons. This is due to the large suppression of fluctuations in iron showers, the ratio of the standard deviation to the mean value of X_{max} is smaller than that for protons, producing smaller values of ξ (see equation (11)). In particular, $\xi_G^{fe} = \xi_G^{pr}/K$ where K increases from ~ 2.3 at $E = 10^{18}$ eV to ~ 2.4 at $E = 10^{19.5}$ eV for QGSJET-II.

3. Conclusions

In this work, we studied in detail statistical bias in the determination of the mean value of X_{max}, suggested in [1], as a possible explanation of the deviation of Auger data from the proton expectation. We used two different functions to fit the X_{max} distribution obtained from simulations: (i) the convolution of an exponential distribution with a Gaussian and (ii) a shifted-Gamma distribution. We find that the bias obtained by using these two functions is more than one order of magnitude smaller than the corresponding one of the exponential distribution, the one used in [1]. We find that the values of the bias, obtained for the convolution of the exponential function with the Gaussian, are larger because it presents a more extended tail to larger values of X_{max} than the shifted-Gamma distribution. We also find that the bias diminishes when a Gaussian (symmetric) uncertainty on the determination of X_{max} is included.

　　　We also calculated the expected bias, as a function of primary energy, using the actual number of events in each energy bin of the Auger data, published in [2], for both hadronic interaction models considered in this work, QGSJET-II and EPOS 1.99. We find that the largest value of the bias, corresponding to the bin with the smallest number of events, is smaller than 1.5 g cm^{-2}, much less than the systematic errors on the determination of $\langle X_{max} \rangle$ estimated in [2].

Appendix A. Parameters for the exp-Gauss fits

The parameters α, β and λ, obtained from the fits of the X_{max} distributions with the exp-Gauss function (see equation (6)), are fitted with linear functions of $\log(E/eV)$ as shown in figure A1. They can be written in the following way:

$$\begin{pmatrix} \alpha(E) \\ \beta(E) \\ \lambda(E) \end{pmatrix} = \begin{pmatrix} C_1 & C_2 \\ C_3 & C_4 \\ C_5 & C_6 \end{pmatrix} \begin{pmatrix} 1 \\ \log(E/eV) \end{pmatrix}, \tag{A.1}$$

where the coefficients C_i, $i = 1 \ldots 6$, are given in table A1 for both hadronic interaction models considered.

Table A1. Coefficients C_i, in (g cm^{-2}), corresponding to QGSJET-II and EPOS 1.99.

|	C_1	C_2	C_3	C_4	C_5	C_6
QGSJET-II	−239.053	51.0096	−18.0164	2.239 81	138.806	−4.575 08
EPOS 1.99	−443.120	63.0078	13.6458	0.320 823	75.2960	−0.987 241

Appendix B. Calculation of ξ for a truncated exponential distribution

It is possible to describe the X_{max} distribution function by a truncated exponential distribution, which is given by

$$P_{TE}(X_{max}) = \begin{cases} \dfrac{1}{\Lambda} \exp\left(-\dfrac{X_{max} - X_c}{\Lambda} \right) & X_{max} \geqslant X_c \\ 0 & X_{max} < X_c \end{cases}, \tag{B.1}$$

where Λ is a parameter that describes the tail of the X_{max} distribution and X_c is the truncation value.

　　　The characteristic function of this distribution is $\phi_{X_{max}}^{TE}(t) = \exp(itX_c)(1-it\Lambda)^{-1}$ and then the characteristic function of the sample mean is given by $\phi_{\bar{X}_{max}^N}^{TE}(t) = \exp(itX_c)(1-it\Lambda/N)^{-N}$,
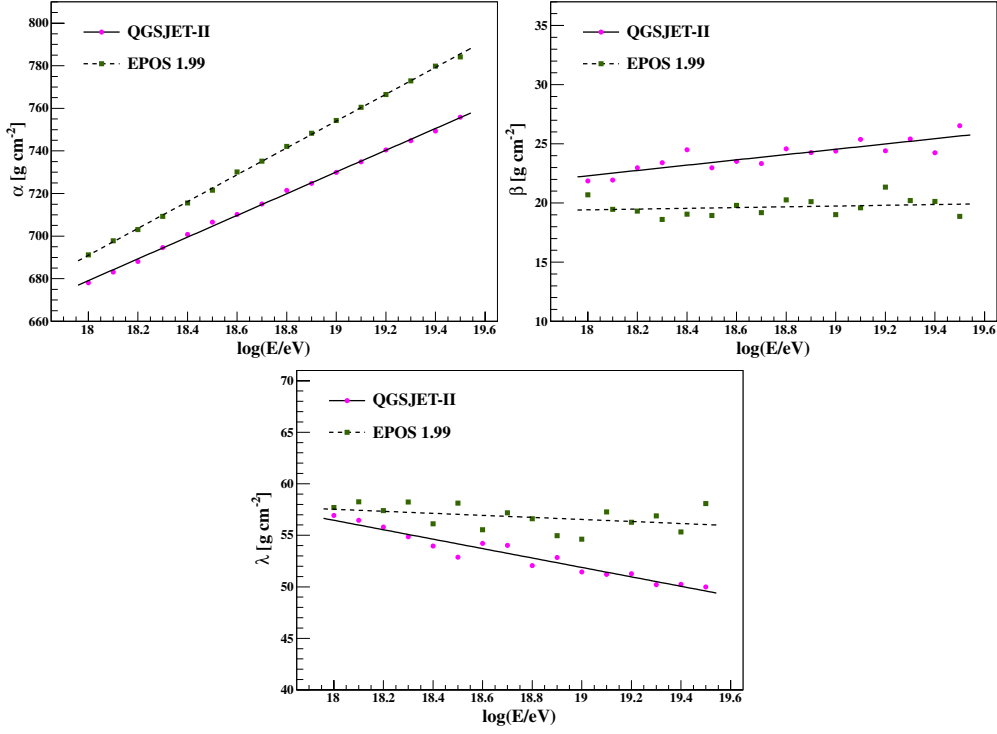
Figure A1. Parameters α, β and λ corresponding to the fits of the $X_{\max}$ distribution with the exp-Gauss function for QGSJET-II and EPOS 1.99. The straight lines correspond to the linear fits of the points.

which corresponds to a shifted Gamma distribution. Therefore, the distribution function of the sample mean is given by

$$\bar{P}_{\mathrm{TE}}\left(\bar{X}_{\max}^N\right) = \begin{cases} \dfrac{\left(\bar{X}_{\max}^N - X_c\right)^{N-1}}{\Gamma(N)\,(\Lambda/N)^N} \exp\left(-\dfrac{X_{\max} - X_c}{\Lambda/N}\right) & \bar{X}_{\max}^N \geqslant X_c \\ 0 & \bar{X}_{\max}^N < X_c \end{cases} \tag{B.2}$$

By using that $\langle X_{\max}\rangle = X_c + \Lambda$, it is easy to show that

$$\xi_{\mathrm{TE}}(N) = \frac{\Lambda}{\Lambda + X_c}\,\frac{1}{N}, \tag{B.3}$$

$$= \frac{\sigma[X_{\max}]}{\langle X_{\max}\rangle}\,\frac{1}{N}. \tag{B.4}$$

Note that, it can be seen, from equation (B.4), that ξ_{TE} takes a very similar form to the one obtained for the shifted-Gamma function, see equation (11).

Typical values of the parameters, obtained experimentally, are $X_c \cong 700$ g cm^{-2} and $\Lambda \cong 56$ g cm^{-2} [10] (note that these parameters depend on primary energy and the ones used here, obtained from [10], correspond to the energy interval $[10^{18}, 10^{18.5}]$ eV, in any case, they are just used to roughly estimate the suppression factor of the bias). Therefore, $\xi_{\mathrm{TE}}(N) \cong 0.125/N$, which is suppressed by a factor 0.125 with respect to the corresponding one to the exponential distribution.

9

References

[1] Wilk G and Wlodarczyk Z 2011 *J. Phys. G: Nucl. Part. Phys.* **38** 085201
[2] Abraham J *et al* 2010 *Phys. Rev. Lett.* **104** 091101
[3] Abbasi R *et al* 2010 *Phys. Rev. Lett.* **104** 161101
[4] Schmidt F, Ave M, Cazon L and Chou A 2008 *Astropart. Phys.* **29** 355
[5] Bergmann T *et al* 2007 *Astropart. Phys.* **26** 420
[6] Ostapchenko S 2006 *Nucl. Phys.* B **151** 143
[7] Pierog T and Werner K 2006 *Phys. Rev. Lett.* **101** 171101
[8] James F 2006 *Statistical Methods in Experimental Physics* (Singapore: World Scientific)
[9] Abraham J *et al* 2010 *Phys. Lett.* B **685** 239
[10] Ulrich R (Pierre Auger Collaboration) 2011 *Proc. 32nd ICRC (Beijing)* vol 5 pp 51–4 arXiv:1107.4804